JOURNAL OF MATERIALS SCIENCE 23 (1988) 1506–1509

High-resolution electron microscopy of solution-grown crystals of poly (*p*-phenylene sulphide)

AKIO UEMURA*, MASAKI TSUJI, AKIYOSHI KAWAGUCHI, KEN-ICHI KATAYAMA
Institute for Chemical Research, Kyoto University, Uji, Kyoto-fu 611, Japan

Crystals of poly (*p*-phenylene sulphide) were obtained from an α-chloronaphthalene solution. The chain axis (the crystal ***c***-axis) was usually normal to the support-film. For these crystals, high-resolution electron microscopic images were taken as the projection of the molecular chains on the ***ab*** plane along the chain axis. Occasionally it was observed that crystals took different orientations on the support-film for undefined reasons. From such orientations, the high-resolution image of a crystal rotated by 28.7° around the ***a***-axis from the usual orientation, was also obtained.

1. Introduction

In the study of the solid state structure of polymers, high-resolution transmission electron microscopy now plays an important role. It visualizes periodical fine structures at an atomic or molecular level and also sometimes gives information on the localized irregular structures such as dislocations. At present, high-resolution images can be obtained comparatively easily as long as polymer specimens are not very sensitive to electron bombardment. For example, the molecular image of poly (*p*-xylylene) (PPX) β-form single crystal is very useful for analysing its crystal structure [1, 2]. Images of edge dislocations in the PPX crystals have also been reported [3]. For polymers with high electrical conductivity, high-resolution images of $(SN)_x$ [4] and poly (*p*-phenylene) [5] have been obtained. In particular, high-resolution electron micrographs of $(SN)_x$ demonstrated that in $(SN)_x$ doped with iodine, iodine atoms settle with some order preferentially in the "skin" region of the $(SN)_x$ fibrils because the region is somewhat disordered in the pristine state [4].

As is well known, poly (*p*-phenylene sulphide) (PPS) is a conducting polymer and its conductivity increases up to 1 $S\,cm^{-1}$ when PPS is doped with AsF_5, a strong electron acceptor [6, 7]. The crystal structure of PPS was analysed by Tabor *et al.* [8] and the unit cell was found to be orthorhombic with the cell dimensions: $\boldsymbol{a}$ = 0.867 nm, $\boldsymbol{b}$ = 0.561 nm and $\boldsymbol{c}$ (chain axis) = 1.026 nm. The morphologies of solution-grown crystals and the crystalline thin films of PPS have already been reported [9]. In this paper we present two kinds of high-resolution images of PPS solution-grown crystal, which are attributed to two different orientations of the crystal. It is worthwhile to observe a crystal with an electron microscope in two or three different directions, because it gives information on the three-dimensional structure of the crystal. Furthermore, if the three-dimensional distribution of dopant in a PPS crystal is known, its conduction mechanism can be better understood.

2. Experimental details

The PPS sample used here was Ryton V-1 manufactured by Phillips Petroleum Company. The crystal was isothermally precipitated from an α-chloronaphthalene solution. The detailed procedure was described in a previous paper [9]. Generally PPS crystallizes from the solution as fibrillar crystals whose long axis corresponds to the ***b***-axis (Fig. 1). The thickness and the width of the fibrillar crystal were evaluated at 11.5 nm by small-angle X-ray scattering and at 100 to 300 nm by electron microscopy at a low magnification, respectively [9]. The electron beam current was measured using a pico-ammeter connected to a Faraday cage. High-resolution images of the crystals were taken on Mitsubishi MEM films at a magnification of 100 000 using Jeol JEM-2000EX (200 kV, C_s = 0.7 mm) or JEM-200CS (200 kV, C_s = 2.8 mm) equipped with a minimum dose system (MDS) [10]. MEM films were developed at 20° C for 5 min with Mitsubishi Gekkol (full strength) or Kodak D-19 (diluted 1 : 1). In order to enhance the periodic structures, the images were processed using the optical filtering method [11].

3. Results and discussion

In taking a high-resolution electron microscopic image, the durability of a crystalline structure against electron irradiation is one of the most important factors. The PPS crystal is comparatively less-sensitive to the electron bombardment, though most other polymer crystals are highly sensitive. Fig. 2 shows the change in lattice spacings with irradiation dose. The lattice spacings are almost invariant with increasing

*Author to whom all correspondence should be addressed.

0022–2461/88 $03.00 + .12

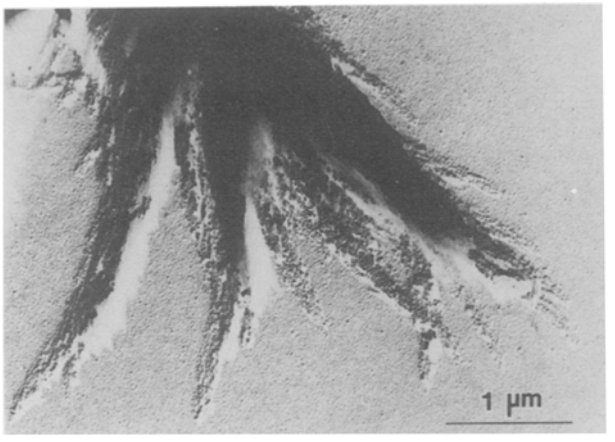

Figure 1 Electron microscopic image of PPS solution-grown crystal shadowed with Pt–Pd. The crystal consists of several fibrillar crystals 100 to 300 nm wide and 11.5 nm thick.

irradiation dose. The total end-point dose (TEPD, the electron irradiation dose needed for crystals to lose crystalline reflections in the diffraction pattern) of the PPS crystal is about 0.2 C cm^{-2} at an accelerating voltage of 200 kV at room temperature. It is about 10 times and about 30 times greater than that of isotactic polystyrene and polyethylene, respectively [12]. Thus we expect high-resolution images, and two types of image attributed to different orientations of the crystal to the support-film were, in fact, obtained.

3.1. N-type

The diffraction pattern shown in Fig. 3a is usually observed from a PPS solution-grown crystal. It basically consists of $hk0$ reflections, i.e. the incident electron beam direction corresponds to the $\langle 0\,0\,1 \rangle$ of the crystal. In other words, the incident electron beam is normal to the basal plane of the crystal and parallel to the molecular chain axis. Extra reflections such as 1 1 1, 2 1 1, etc., very often appear as in Fig. 3a. The appearance of these reflections is explained by the assumption that PPS fibrillar crystals change their orientation by twisting around the ***b***-axis (the long axis of a fibrillar crystal is in the ***b***-axis direction) [9]. However, because the extra reflections are weaker than $hk0$, the image corresponding to this electron diffraction pattern is expected to be mainly the projection of individual molecular chains on the crystal ***ab*** plane along the chain axis. The crystal orientation in question corresponds to Fig. 4a.

According to the results of crystal structure analysis of PPS [8], in a unit cell there are two molecular chains and a chain has two monomer units (S–C_6H_4), i.e. there are four monomer units in a unit cell, and each monomer unit has one phenylene group. The planes of a phenylene group are set alternately at $+45°$ and $-45°$ against the (1 0 0) plane by rotating around S–C_6H_4–S bonds [8]. Four phenylene groups in the unit cell have different orientations to one another. For both molecular chains, the centres of the phenylene groups included in the same molecular chain overlap in the projection on the ***ab*** plane along the ***c***-axis, as seen in the Fig. 4a. In the high-resolution image, it is expected that both molecular chains in a unit cell will be seen as the same ellipse-like shape.

Fig. 5a shows an image which was processed using the optical filtering method in order to enhance the periodic structure in the original micrograph. The inset (lower left-hand corner) of Fig. 5a shows the optical diffraction pattern obtained by optical transform of the original negative. This optical diffraction pattern resembles well the electron diffraction pattern (Fig. 3a). It is, however, not arcing because it is obtained from a small coherent region in the crystal. From a detailed analysis of the optical diffraction pattern, it was confirmed that the fringes recorded on the negative were assigned to 2 0 0 (0.434 nm in spacing), 1 1 0 (0.471 nm) and $\bar{1}\,1\,0$ (0.471 nm) and, as expected, the image just corresponded to the projection of PPS crystal on the ***ab*** plane along the ***c***-axis. In the processed image of Fig. 5a, each dark ellipse corresponds to a single molecular chain projected on the ***ab*** plane along the chain direction as mentioned above. Taking account of the parameters of the crystal structure and the characteristics of the electron microscope, e.g., the spherical aberration coefficient (C_s = 2.8 mm), the amount of defocus (Δf = 90 nm, positive for under focus), the molecular image projected along the chain axis was simulated by a computer on the assumption of kinematical diffraction [13]. The

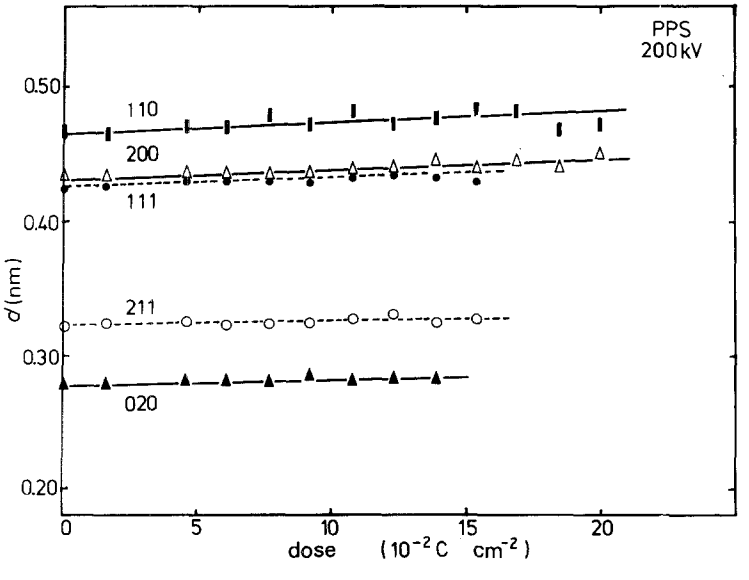

Figure 2 Change in lattice spacings with electron irradiation dose at 200 kV at room temperature. The lattice spacings are almost invariant with increasing irradiation dose. TEPD is about 0.2 C cm^{-2}.

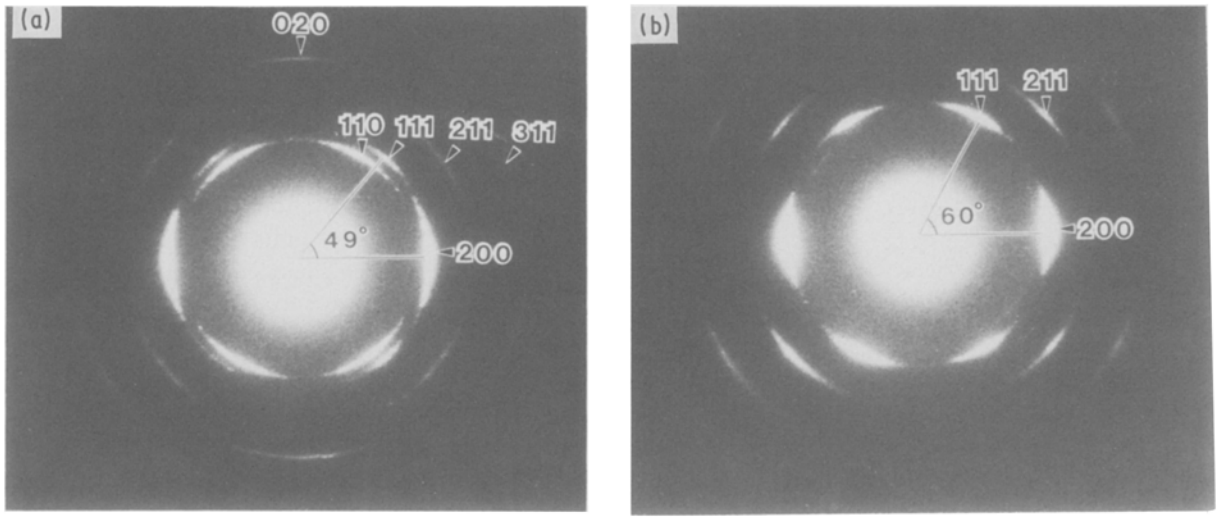

Figure 3 Electron diffraction patterns of a solution-grown crystal. Pattern (a) is usually observed and basically consists of $hk0$ reflections (N-type). Pattern (b) is occasionally observed and consists of $h00$ and $h11$ reflections (T-type). The angles between the lines drawn from the origin to the centres of 200 and 111 reflections are 49° in (a) and 60° in (b).

simulated image shown at the upper right-hand corner of the Fig. 5a coincides well with the electron microscopic image.

3.2. T-type

The diffraction pattern shown in Fig. 3b is occasionally observed in solution-grown crystals of PPS. It reveals the $h00$ and $h11$ reflections. It should be noted that in Fig. 3, the angles between the lines drawn from the origin to the centres of 200 and 111 reflections is 60° in (b), in contrast to 49° for N-type in (a). In the case of Fig. 3b, the crystal is rotated by 28.7° around the ***a***-axis from the N-type orientation. In other words, the incident electron beam direction has changed from the $\langle 001 \rangle$ direction (N-type) to the $\langle 0\bar{1}1 \rangle$ direction of the crystal.

Fig. 4b illustrates the projection of the crystal along the $\langle 0\bar{1}1 \rangle$ direction. In this case, none of the four monomer units in one unit cell overlap with the other monomer units, but they do overlap with monomer units located on the equivalent positions in other unit cells along the $\langle 0\bar{1}1 \rangle$ direction. In the rectangular area indicated in Fig. 4b there are four monomer units which are different in orientation, and they are grouped into two classes with respect to their projected shape; A and B. The high-resolution image of this orientation of the crystal was also obtained.

Fig. 5b shows the image processed by optical filtering. The inset at the lower left-hand corner of Fig. 5b shows the optical diffraction pattern obtained from the original negative. Though this optical diffraction pattern is also spotty as in the case of N-type, it resembles the electron diffraction pattern quite well (Fig. 3b). From this optical diffraction pattern it was confirmed that the fringes recorded on the negative are 200, 111 (0.428 nm), $\bar{1}11$ (0.428 nm), 211 (0.325 nm), $\bar{2}11$ (0.325 nm) lattice fringes. In A (Fig. 4b), where a phenylene group is set almost in the "edge-on" position, carbon atoms of a phenylene group come together and sulphur atoms are located close to a phenylene group. On the other hand, carbon atoms of a phenylene group are not so condensed in B, because a

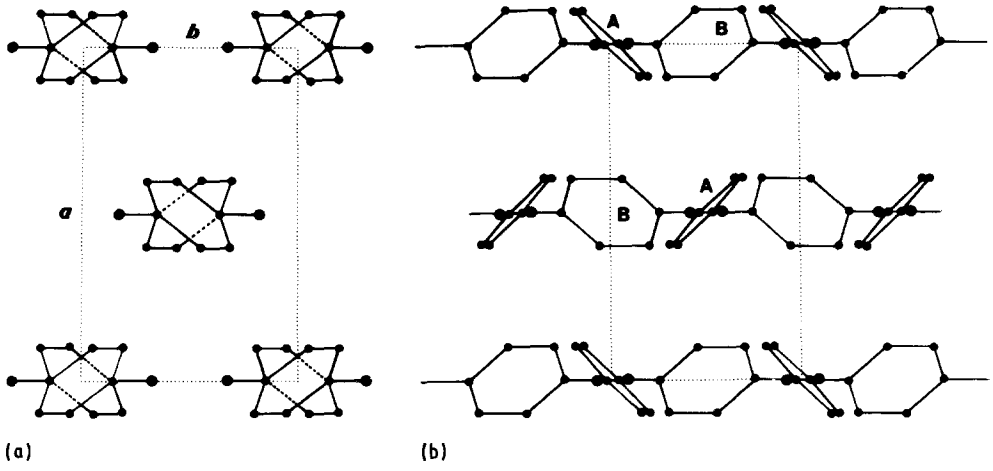

Figure 4 Projections of the crystal structure of PPS. Projection (a) is for the $\langle 001 \rangle$ incidence of the electron beam into the crystal and projection (b) is for $\langle 0\bar{1}1 \rangle$. Phenylene groups in a chain in a unit cell are set alternately at $+45°$ and $-45°$ against the (100) plane by rotating around S–C_6H_4–S bonds. In (a) the centres of the phenylene groups in a chain overlap each other. In the rectangular area indicated in (b), there are four projected monomer units which are different in orientation. In A, a phenylene group is set almost in an "edge-on" position, and in B, almost in a "flat-on" position. (●) S atom, (•) C atom. Hydrogen atoms are not shown. The $\langle 011 \rangle$ incidence is identical to the $\langle 0\bar{1}1 \rangle$ incidence in projection.

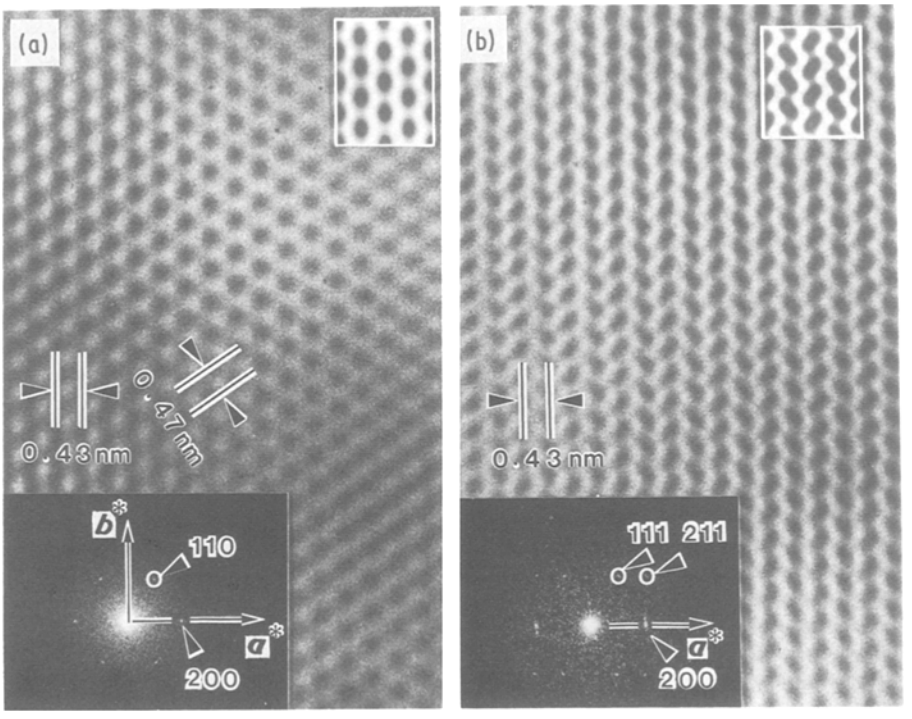

Figure 5 High-resolution electron microscopic images (× 100 000) taken at an accelerating voltage of 200 kV. Image (a) is for the $\langle 0\,0\,1 \rangle$ incidence and (b) is for $\langle 0\,\bar{1}\,1 \rangle$. In both, the optical diffraction pattern is given at the lower left-hand corner and the simulated image at Scherzer focus is at the upper right-hand corner. In (a), each dark ellipse corresponds to a single molecular chain projected on the ***ab*** plane in the chain direction. In (b), each dark ellipse corresponds to A in Fig. 4b and a region between ellipses corresponds to B.

phenylene group appears nearly in a "flat-on" orientation, and sulphur atoms are far from the phenylene group. From above, it is considered that each dark ellipse of Fig. 5b corresponds to A and the region between ellipses corresponds to B, because in the high-resolution electron microscopic images the part packed densely with atoms should appear as the dark part, according to the image simulation at the optimum (Scherzer) focus [14]. The simulated image (inset, upper right-hand corner of Fig. 5b) by a computer using $C_s = 0.7$ mm and $\Delta f = 48$ nm (Scherzer focus) for JEM-2000EX coincides well with the electron microscopic image (Fig. 5b), and proves that the above consideration is reasonable.

4. Conclusion

We have obtained two kinds of high-resolution electron microscopic images of PPS solution-grown crystal, attributed to two different orientations of the crystal. The images were obtained using the $\langle 0\,0\,1 \rangle$ and $\langle 0\,\bar{1}\,1 \rangle$ incident electron beam directions, respectively. From the latter, it was confirmed that the two phenylene groups in a molecular chain in a unit cell have different orientations. The result supports directly the structure analysis by Tabor *et al.* [8]. High-resolution images of a crystal in two different crystallographic directions are very useful in determining the three-dimensional structure and also to study the three-dimensional distribution of the dopant relating to the position of polymer chains in the doped PPS crystal. Such an investigation is in progress.

Acknowledgement

The authors thank Mr K. Shibatomi, Jeol Ltd, for his help in taking high-resolution images using a JEM-2000EX.

References

1. M. TSUJI, S. ISODA, M. OHARA, A. KAWAGUCHI and K. KATAYAMA, *Polymer* **23** (1982) 1568.
2. S. ISODA, M. TSUJI, M. OHARA, A. KAWAGUCHI and K. KATAYAMA, *ibid.* **24** (1983) 1155.
3. *Idem, Makromol. Chem. Rapid Commun.* **4** (1983) 141.
4. A. KAWAGUCHI, S. ISODA, J. PETERMANN and K. KATAYAMA, *Colloid Polym. Sci.* **262** (1984) 429.
5. A. KAWAGUCHI, M. TSUJI, S. MORIGUCHI, A. UEMURA, S. ISODA, M. OHARA, J. PETERMANN and K. KATAYAMA, *Bull. Inst. Chem. Res. Kyoto Univ.* **64** (1986) 54.
6. J. F. RABOLT, T. C. CLARKE, K. K. KANAZAWA, J. R. REYNOLDS and G. B. STREET, *J. Chem. Soc. Chem. Commun.* (1980) 347.
7. R. R. CHANCE, L. W. SHACKLETTE, G. G. MILLER, D. M. IVORY, J. M. SOWA, R. L. ELSENBAUMER and R. H. BAUGHMAN, *ibid.* (1980) 348.
8. B. J. TABOR, E. P. MAGRÉ and J. BOON, *Eur. Polym. J.* **7** (1971) 1127.
9. A. UEMURA, S. ISODA, M. TSUJI, M. OHARA, A. KAWAGUCHI and K. KATAYAMA, *Bull. Inst. Chem. Res. Kyoto Univ.* **64** (1986) 66.
10. Y. FUJIYOSHI, T. KOBAYASHI, K. ISHIZUKA, N. UYEDA, Y. ISHIDA and Y. HARADA, *Ultramicroscopy* **5** (1980) 459.
11. M. TSUJI, S. ISODA, M. OHARA, K. KATAYAMA and K. KOBAYASHI, *Bull. Inst. Chem. Res. Kyoto Univ.* **55** (1977) 237.
12. M. TSUJI, A. UEMURA, M. OHARA, A. KAWAGUCHI, K. KATAYAMA and J. PETERMANN, *Sen-i Gakkaishi* **42** (1986) T-580.
13. K. ISHIZUKA and N. UYEDA, *Acta Crystallogr.* **A33** (1977) 740.
14. O. SCHERZER, *J. Appl. Phys.* **20** (1949) 20.

Received 27 April
and accepted 6 July 1987